Using a Piezo-Resistive Tactile Sensor for Detection of Incipient Slippage

Matthias Schöpfer, Carsten Schürmann, Michael Pardowitz and Helge Ritter
Bielefeld University, Bielefeld, Germany

Abstract

The detection of incipient slip is an important cornerstone in tactile based grasping. In this paper, we present an approach to detect incipient slip using a fast piezo-resistive, yet static tactile sensor pad. Our approach renders special slip sensors obsolete and therefore enables static and dynamic sensing with one sensing mechanism. For the detection of the slip, a fast fourier transform is used to pre-process the data. In a subsequent step, a standard artificial neural net is trained on the data from the frequency domain to detect slippage, as well as to discriminate different surface textures.

1 Introduction

A great challenge in robotics research today is human like grasping. Humans are able to grasp unknown objects, matching the applied force carefully to the load needed to lift, handle and manipulate the object. This is done through the detection of micro-slips of the object. These micro-slips produce vibrations, which the human skin is able to sense and use in the active motor control of the fingers. With the information of incipient slip, the optimal force for objects can easily be determined and a force closure grasp can be established [6, 15]. To detect these micro-slips with artificial systems, special dynamic tactile sensors have been designed (e.g. [14, 12]), many of them using the piezo-electric effect. Those sensors yield a good dynamic response and good results for the purpose of slip detection. Unfortunately though, the downside of these sensors is, that they sometimes can be easily damaged and above all, are not suited for measuring static or constant forces. While the human skin uses four different kinds of mechanoreceptors for different aspects of tactile sensing submodalities, it remains a challenge to integrate static and dynamic sensors in an artificial sensing device. Especially, the avoidance of blind spots, minituarisation and a low amount of cabling are main challenges in the tactile sensor design.

Combinations of static and dynamic sensors have been successfully integrated into a robotic hand [3] providing slip detection. Recently, new sensors which specifically addressing the problem of detecting slippage have been designed [13, 16, 7]. The practical use of slippage information in a grasping task can be seen in [4], where a controller adjusts the grasp force with the use of a slip sensor.

In contrast to the mentioned work, in this paper a piezo-resistive, and therefore static tactile sensor is used to detect incipient slippage. A set of five different objects with different surface texture is used as a test and training set. For the data acquisition, the objects are fixed and the sensor is moved in a sliding motion over the object. To ensure a precise motion, the sensor is mounted on a Kuka Light Weight Robot (LWR). The recorded data is used to learn the detection of slippage as well as to distinguish between different object surfaces.

2 Experimental Setup

Our tactile robotic setup consists of two Kuka LWR arms in a bi-manual setup, as can be seen in **Figure 1**. This way, grasping with the tactile pads, or the versatile manipulation of deformable material is possible [8]. The experimental setup for this experiment was mono-manual and consisted of a tactile sensor module mounted on a Kuka LWR as in **Figure 2**.

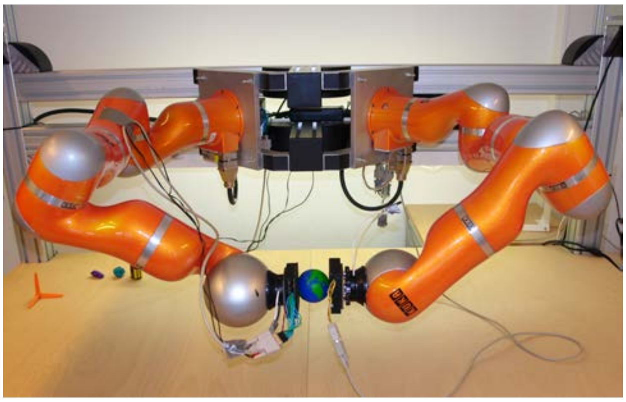

Figure 1: The bi-manual setup in the tactile lab. Both Kuka LWRs have a myrmex tactile sensor mounted on their end effectors. Both sensors have magnetic connectors which act as predetermined breaking points in case of accidentally high contact forces.

2.1 Tactile Sensor

The tactile sensor employed is named "myrmex" and was developed to enable very high speed data acquisition in hand with high sensibility for low contact forces [9]. A myrmex sensor is a square module of dimensions 80 $[mm]$

x 80 [mm] with a height of 15 [mm]. The sensor's working principle is based on the resistive method to measure pressure on a surface. For this method a conductive elastomer is used, which changes its resistance proportional to pressure applied to it. The change in resistance behaves well over a large range (almost linear in its responsiveness), with non-linear responses only at low and very high pressures. Each myrmex sensor has a matrix of 16 x 16 sensor cells on its surface, resulting in a resolution of 5 [mm] x 5 [mm]. These sensor cells get covered with an carbonized foam which functions as the conductive elastomer. One strength of this approach is that there are no measurement gaps between the sensor cells. Thus, the complete sensor area is sensitive to contact forces.

The sensitivity and range of pressure detected is very dependent on the properties of the foam which is used. Forces below 0.1 [g/mm^2] and as high as 20 [g/mm^2] can be measured with the appropriate foam. The myrmex sensors are designed to also function in a big array of modules. It is possible to enlarge the sensing area by simply sticking two modules together. Arbitrary configurations can be used this way. However, in this paper, the sensor was used in the standalone mode.

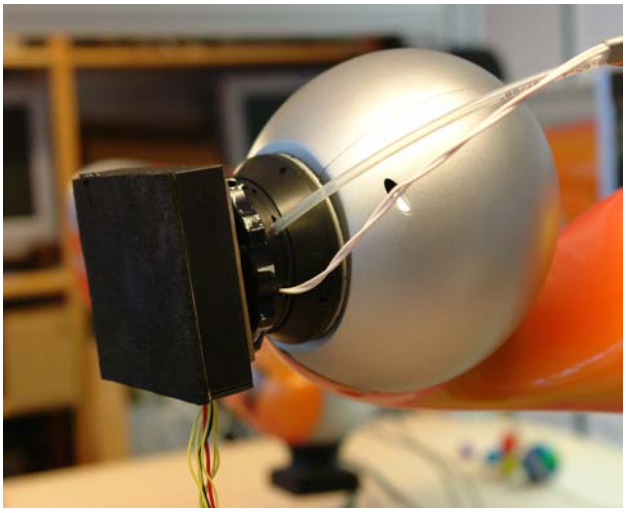

Figure 2: The myrmex sensor mounted on the Kuka LWR end effector. The internal cabling (air and power) that can be seen in the picture are not used in this setup

In this single or standalone operation, it can sample its surface at about 1800 [Hz]. Each of the 256 sensor cells on a module returns a digital value with a resolution of 12 Bit. Each sensor module is equipped with a PIC32 microcontroller which is responsible for acquiring the data from each cell and storing it prior to transmission. The modules are normally interconnected with pin headers and use a custom made parallel protocol to transmit the data between each other. This protocol allows to identify the connections between the units and to determine an modules location inside a matrix of such modules. This implementation was chosen so that an array of these modules can be arranged with a varying number of modules and different rectangular shapes without modifying the hard- or firmware. Because there are no compatible or standardized version of this protocol for normal PCs, a module array or single module gets connected to a mediator unit which then transfers the tactile data to a PC. This mediator unit is equipped with an AVR32 microcontroller, which communicates with the sensor(s) via the sensors own parallel protocol. The mediator uses an USB 2.0 high speed controller to communicate with a PC. The USB connection was chosen because it provides high enough bandwidth for high speed data acquisition even with many modules, and offers a standardized protocol which is very suitable for the task: the USB Video Class. By making use of the USB video protocol, the data from the modules is packaged in a video frame with the sensor cell values encoded as pixel data. This allows a very convenient translation to the variable array sizes into the frame dimensions which then can be easily be interpreted by the PC software. The biggest advantage of the USB video protocol is its standardization and the availability of low level drivers for this device class.

2.2 Kuka LWR

The Kuka Light Weight Robots have torque sensors in every joint. The Kuka robot facilitates these torque readings to allow different modes of impedance control. For the task at hand, one robot was set into Cartesian impedance control, where it is possible to set different stiffness and damping parameters for each of the Cartesian dimensions.

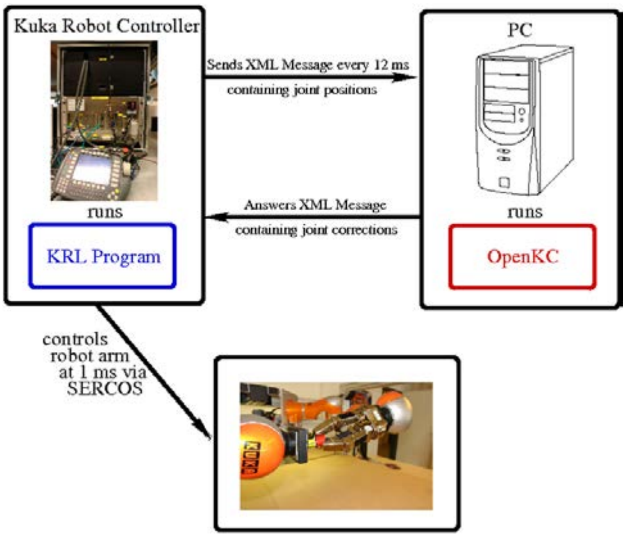

Figure 3: Control Scheme of the Kuka LWR using the RSI XML interface. The XML messages are send over Ethernet and allow real time controll over the Kuka Robot

Also the robot provides a force estimation for the end effector. The forces on the end effector are calculated with the use of a dynamic model of the robot and the torque readings within the Kuka controller [1]. The force estimation is used to establish an ongoing contact force between the myrmex sensor (which is mounted on the end effector) and the material probe.

The robot arm is controlled in real-time using Kukas RSI-XML interface on the robots side and our own implementation of the provided interface of the controlling server, the OpenKC software package. The communication between the robot controller and, in out case, a PC running a highly preemptive Linux kernel, is done via TCP/IP over Ethernet. The robot sends an XML message with its actual positions, torques and estimated forces, the server software reads out the transmitted data and will send a response packet to the robot controller. In the response packet, a correction for either the joint values or the Cartesian position is send to the robot. The robot will generate packets in a 12 [ms] interval, and the server needs to answer within this time period. An overview of the architecture can be found in **Figure 3**.

The Cartesian correction mode does not allow the generation of movements that take advantage of the redundant joint of the robot. The inverse kinematics on the Kuka controller is up to the date of writing not able to take advantage of the additional degree of freedom. Also, since the Kuka controller will always have its own inverse kinematics running in RSI-XML mode, it is not possible to drive the robot through a (6-DOF) singular configuration, even when the robot is controlled in joint space.

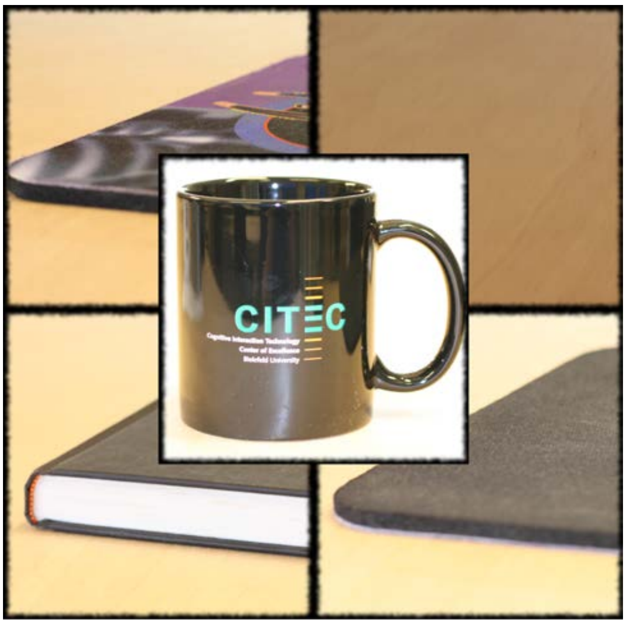

Figure 4: The five objects that were probed, smooth side of a mouse pad, a wooden surface, the cover of a book, the rough side of a mouse pad as well as a ceramic cup.

To do Cartesian space control and at the same time taking advantage of the redundant DOF, we use a C++ implementation of the Control Basis Framework [5, 2]. This framework provides flexible means to synthesize closed loop controllers from simple components: Artificial potential functions, sensor transforms, effector transforms and resources.

Sensor transforms map actuator sensor readings (joint positions) into the task space of interest (e.g. Cartesian space).

Additionally the control basis framework allows for hierarchical composition of controllers. This is achieved by means of manipulator Jacobian null space projection [11]. We use in our use case a subordinate controller which will avoid singular configurations and joint limits.

3 Experiments

To have a sound data basis for the slip detection algorithm, the described setup was used to record a number of stick/slip conditions. A total of five different surfaces (cf. **Figure 4**) was probed: a book cover, a wooden surface, a ceramic cup, the smooth surface of a mouse pad and the rough rubber side of the mouse pad.

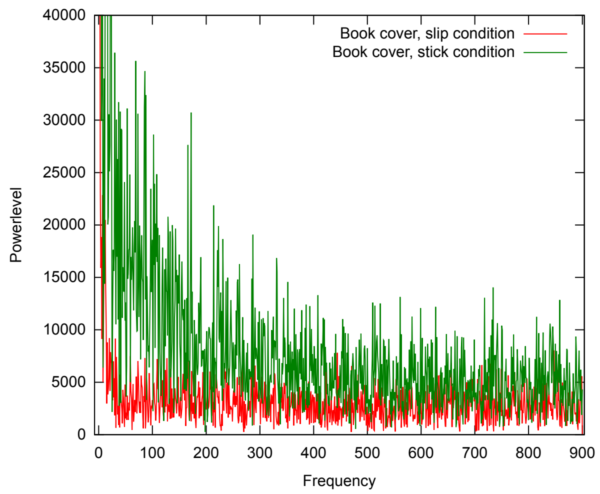

Figure 5: The graph shows the spectrum of two samples. Both samples come from the same experiment. The sampled object is the book cover. A clear distinction between a slip and stick condition can be made.

Each object was sampled five times. During the sampling procedure, at first, contact with the object was established and a contact force of 0.8 $[N]$ was maintained. Afterward, the end effector was moved to three further positions on the material. The positions were aligned in a square, with a short resting phase of approximately one second at each corner. In a subsequent run, the same square was sampled while maintaining a force of 2 $[N]$. During the run, the tactile data from the myrmex sensor as well as the position and force information of the robot were recorded. The recording frequency was run in sync with the robots interpolation cycle at 83 $[Hz]$. The software to record the myrmex tactile data run in a parallel thread saving all tactile frames coming from the sensor. Therefore it was possible, for each frame recorded in sync with the robots update frequency, to tag the last 1800 tactile frames to the robots movement during this cycle.

3.1 Data Processing

Each recorded sample (tactile data and robot movements) was processed as one data point. To transfer the tactile time series from the time to the frequency domain, a one dimensional fast Fourier transform (FFT) was done. The FFT is an efficient way to compute the discrete Fourier transform of a given data set. Since we are looking at finite length signals and different window length - which naturally limits the Nyquist frequency - leakage and aliasing effects have to be taken into account. Also the rubber foam of the myrmex sensor impairs the analysis of the "true" spectrum [10]. Despite these limitations, a qualitative and quantitative differences in the spectrum between slip and stick conditions can be found. In **Figure 5** the frequency spectrum of a stick and a slip condition is shown as a typical example. In this case, the disparity is evident, it has to be said though that with other samples and materials the differences are sometimes not that clear anymore.

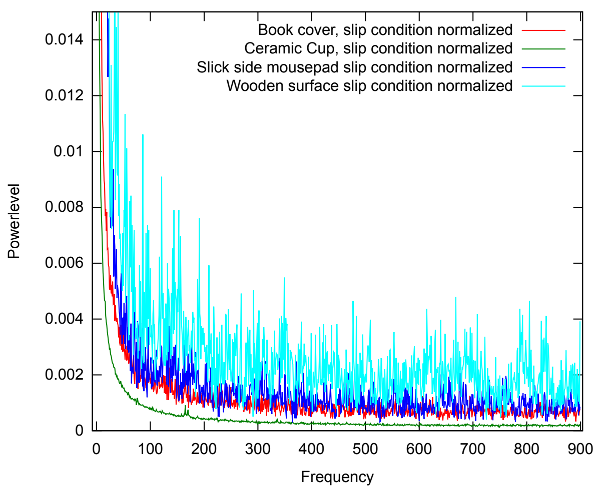

Figure 6: In this graph, the averaged and normalized frequency spectra of different surfaces are exemplary shown. To enhance the readability only four of the five different materials are displayed.

The frequency spectra of the different materials during slip give cause to the assumption that a material classification of the surface, although a challenge, can be done. The normalized and averaged power levels of the different materials during slip can be seen in **Figure 6**.

3.2 Classification Architecture

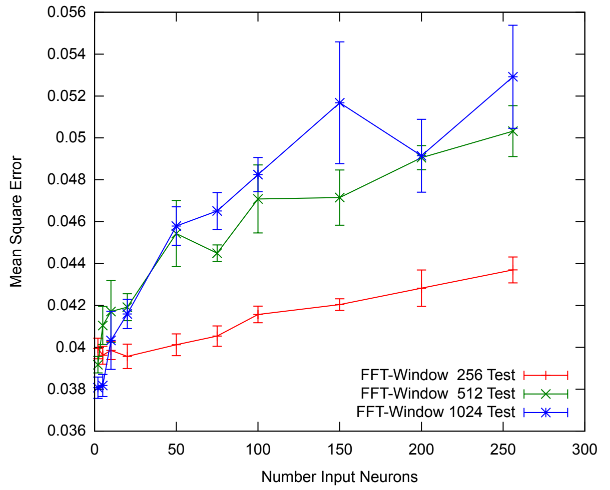

Figure 7: Classification results for different window sizes w and number of input neurons n.

To show the feasibility of our approach and the ability of the tactile sensor pad to serve as a conjunction of a static and a dynamic tactile sensing device, a standard artificial neural net was trained to detect slippage. A first parameter of this approach is the window size w of the FFT as it has impact on the frequencies that are detectable and the possible input dimension. In a subsequent step, the resulting spectrum was divided into n frequency bands of equal size. Also, the input had to undergo a normalization step, where two different methods were tested: a predetermined constant scaling factor and a "dynamic" normalization with the "DC" element (the Null-frequency part) of the FFT. In the following, normalized will refer to the dynamic normalization. If not stated elsewise, a constant scaling was done. If not stated different, a n–20–1 neural net was used. The answer of the neural net is the (estimated) slipping velocity.

4 Results

4.1 Slip Detection Task

The recorded data was arbitrarily divided into a training and a test set. For the window size w, the values 256, 512 and 1024 were tested, for the number of frequency bands and therefore the number n of inputs. A total of ten different values for n in the range 2..256 where used. For each set of parameters, five randomly initialized neural nets were trained and then tested. For all results, the mean square error (MSE) was calculated:

$$MSE(\overline{X}) := \frac{1}{n}\sum_{i=1}^{n}(f(x_i) - y_i)^2 \qquad (1)$$

The error on the test data set showed not to benefit from values $n \geq 20$. Obviously, the additional neurons on the input layer lead to over-fitting effects which have a negative impact on the test error (cf. **Figure 7**).

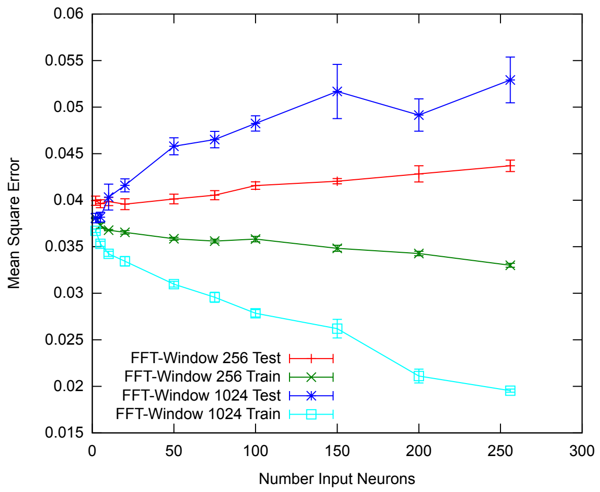

Figure 8: Classification results including training and test errors for different window sizes w.

In **Figure 8** a comparison of the training and testing set with different window sizes can be seen. A larger window size significantly improves the classification rate on the training set, but at the same time reduces the generalization of the net.

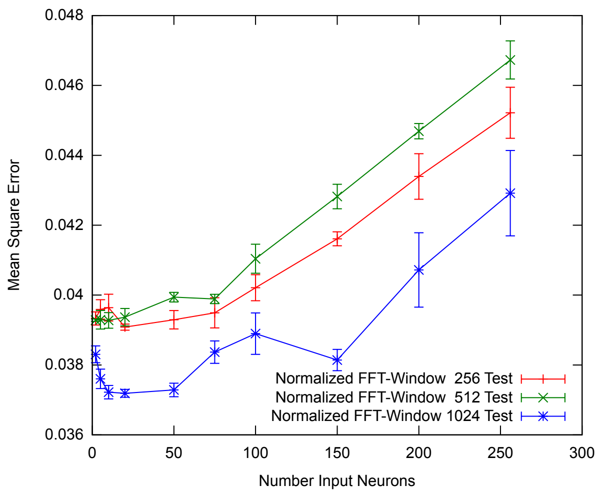

Figure 9: The five objects that were probed, smooth side of a mouse pad, a wooden surface, the cover of a book, the rough side of a mouse pad as well as a ceramic cup.

Interestingly the results for the dynamic normalization reverse the previous findings. While for the window size of 256 and 512 samples almost equal error rates, the best results are at a window size of 1024. Also, the classification error is overall lower than in the fixed factor normalization. For details, see **Figure 9**.

4.2 Material Classification Task

For the material classification task a n-15-5 neural net was used, with the window size w fixed at 1024. Although perfect classification on the training set could be obtained, the test error was unsatisfactory. In **Figure 10** the test results are summarized.

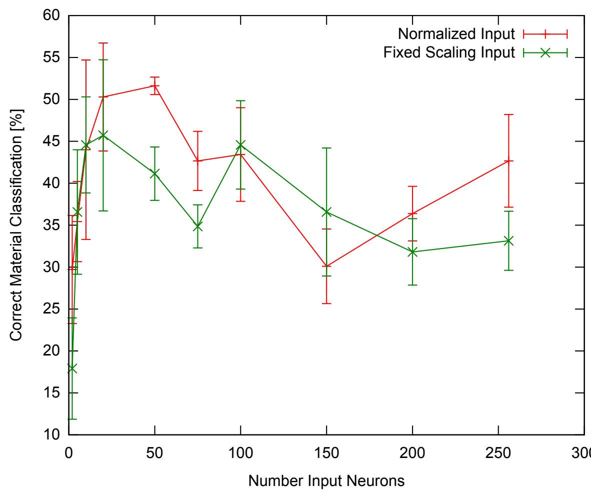

Figure 10: In this graph the correct classifications of the material surface texture are plotted. In this even for humans difficult task, a good generalization could not be achieved.

When taking a closer look at the confusion matrix, which can be found in **Table 1**, one can find that very distinct surfaces like the ceramic cup, which is significantly smoother than all the other surfaces, is classified quite well.

	book	mp rh	mp sh	cup	wood
book	8.5%	0%	1.0 %	2.8 %	12.4 %
mp rough	1.9 %	18.0 %	8.5 %	0.0 %	0.0 %
mp smooth	0.0 %	9.5 %	8.5 %	0.0 %	1.9 %
cup	0.0 %	0.0 %	0.0 %	6.6%	0.0 %
wood	0.0 %	0.0 %	11.4 %	0.0 %	8.5 %

Table 1: Confusion matrix of the material classification task. The rows represent the answer from the neural net whereas the columns stand for the true class. The diagonal entries are the correct classifications.

5 Conclusions and Outlook

The authors presented a piezo-resistive high-speed tactile sensor pad (myrmex) that enables researchers to sense static and dynamic tactile events. To demonstrate the variability of the sensor, a method to detect incipient slippage of objects on the sensor was illustrated. This task is found to be important to solve tactile based grasping of unknown objects. It could be shown that through a discrete Fourier transform, a neural net was able to estimate the slippage (velocity) of different objects.

Overall, a set of five different objects with different surface textures and friction were sampled using a Kuka LWR with the myrmex sensor mounted at the robots end effector. The applied force was controlled through the robots intrinsic torque sensors. The objects were fixed so that movement of the robot on the object could be interpreted as slip event. Also the applied force was varied.

Using a similar approach, the classification of object surfaces as a rough estimate was presented. To improve the recognition of different textures are one of the future goals of the authors. It must be stated, that the task is quite challenging, since the used surfaces can even by humans be easily be confused.

For future research, grasp experiments with the slip detection as a grasp force controller are planned. If those experiments show to be promising, the integration of the sensors in a robotic gripper or hand would be a logical implication.

Acknowledgment

This work was supported by the Excellence Cluster EXC 277 Cognitive Interaction Technology. The Excellence Cluster EXC 277 is a grant of the Deutsche Forschungsgemeinschaft (DFG) in the context of the German Excellence Initiative.

References

[1] A. Albu-Schaffer and G. Hirzinger, *Parameter Identification and Passivity Based Joint Control for a 7DOF Torque Controlled Light Weight Robot* , Proc. IEEE Int'l Conf. on Robotics and Automation 2001, 2001, pp. 2852–2858.

[2] O. Brock, A. Fagg, R. A. Grupen, R. Platt, M. Rosenstein, and J. Sweeney, *A framework for the development of robot behavior*, The International Journal of Humanoid Robotics **2** (2005), no. 3.

[3] D. Groeger, N. Gorges, and H. Woern, *Tactile sensing for an anthropomorphic robotic hand: Hardware and signal processing*, Proc. IEEE International Conference on Robotics and Automation, ICRA, 2009, pp. 895 – 901.

[4] D. Gunji, Y. Mizoguchi, S. Teshigawara, A.Ming, A. Namiki, M. Ishikawaand, and M. Shimojo, *Grasping force control of multi-fingered robot hand based on slip detection using tactile sensor*, Proc. IEEE International Conference on Robotics and Automation, ICRA, 2008, pp. 2605 – 2610.

[5] Manfred Huber and Roderic A. Grupen, *Learning to coordinate controllers - reinforcement learning on a control basis*, In Proceedings of the International Joint Conference on Artificial Intelligence, 1997, pp. 1366–1371.

[6] R. S. Johansson and G. Westling, *Roles of glabrous skin receptors and sensorimotor memory in automatic control of precision grip when lifting rougher or more slippery objects*, Experimental Brain Research **56** (1984), 550–564.

[7] K.-M. Lee and S. Foong, *Lateral optical sensor with slip detection of natural objects on moving conveyor*, Proc. IEEE International Conference on Robotics and Automation, ICRA, 2008, pp. 329 – 334.

[8] Matthias Schöpfer, Carsten Schürmann, Florian Schmidt, Michael Pardowitz, and Helge Ritter, *Handling of deformable material using tactile sensors in a bi-manual scenario*, Tactile sensing in Humanoids – Tactile Sensors and beyond @ IEEE-Ras Conference on Humanoid Robots (Humanoids) (2009).

[9] Carsten Schürmann, Robert Haschke, and Helge Ritter, *Modular high speed tactile sensor system with video interface*, Tactile sensing in Humanoids – Tactile Sensors and beyond @ IEEE-Ras Conference on Humanoid Robots (Humanoids) (Paris, France), 06/12/2009 2009.

[10] Makoto Shimojo, *Mechanical filtering effect of elastic cover for tactile sensor*, IEEE Transactions on Robotics and Automation (1997), no. Vol.13, No. 1.

[11] Bruno Siciliano, *Springer handbook of robotics*, Springer, Berlin, 2008 (ger).

[12] J. S. Son, E.A. Monteverde, and R. D. Howe, *A tactile sensor for localizing transient events in manipulation*, Proc. IEEE International Conference on Robotics and Automation, ICRA, 1994, pp. 471–476.

[13] S. Teshigawara, K. Tadakuma, A. Ming, M. Ishikawa, and M. Shimojo, *Development of high-sensitivity slip sensor using special characteristics of pressure conductive rubber*, Proc. IEEE International Conference on Robotics and Automation, ICRA, 2009, pp. 3289 – 3294.

[14] M. E. Tremblay and M. R. Cutkosky, *Estimating friction using incipient slip sensing during a manipulation task*, Proc. IEEE International Conference on Robotics and Automation, ICRA, 1993, pp. 429–434.

[15] G. Westling and R.S. Johansson, *Factors Influencing the Force Control During Precision Grip*, Experimental Brain Research **53** (1984), 277–284.

[16] H. Yussof, J. Wada, and M. Ohka, *Object handling tasks based on active tactile and slippage sensation in a multi-fingered humanoid robot arm*, Proc. IEEE International Conference on Robotics and Automation, ICRA, 2009, pp. 502 – 507.